RSC Advances

RSCPublishing

Disproportionation route to monodispersed copper nanoparticles for the catalytic synthesis of propargylamines†

Huizhang Guo,[a] Xiang Liu,[a] Qingshui Xie,[a] Laisen Wang,[a] Dong-Liang Peng,*[a] Paula S. Branco[b] and Manoj B. Gawande*[b]

By taking advantage of the coordination between a monovalent Cu^+ precursor and trioctylphosphine, monodisperse Cu nanoparticles were synthesized *via* a disproportionation reaction. A Cu@SiO₂ nanocatalyst was formed by supporting Cu nanoparticles onto a silica aerogel, which showed a high surface area (779.53 m^2 g^{-1}) and excellent catalytic activity for the synthesis of propargylamines.

Well-defined nanostructures have emerged as versatile alternatives in the fields of science and technology, especially in catalysis.[1] These nanocatalysts have been extensively employed in various catalytic processes[2,3] and environmental remediation,[4] as well as magnetically separable nanocatalysts.[5] Among these, supported nanocatalysts have been explored extensively by chemists, because of their significant contribution to the field of nanocatalysis. Various transition metal nanostructures have been studied and employed for several applications. Since the emergence of nanotechnology, Cu nanostructures have shown a variety of applications ranging from conductive features in electronic devices[6–9] to catalysis.[10–13] Meanwhile, copper nanostructures have shown a great potential to replace noble metals such as Ag and Au in many fields as they are inexpensive. However, compared to their noble metal counterparts (namely, Pt,[14] Au,[15] and Ag[16]) which have been successfully synthesized with various morphologies, the preparation of Cu nanocrystals has not been equally successful.[13,17] The reduction of the hitherto considered difficult transition metals such as Ni, Cu and Co nanocrystals in solution requires strong reducing agents and high temperatures because of their relatively low redox potential.[7] Contradictorily, control of the nucleation and

growth of the Cu nanocrystals would be lost in the presence of these strong reducing conditions.[18] Therefore, for the synthesis of monodisperse Cu nanoparticles in solution, it is imperative to focus our attention towards the mechanism by which Cu ions are reduced into zero-valent Cu(0) atoms and controlling the nucleation and growth rate with stabilizing agents.[19]

Controllable synthesis of monodisperse Cu nanoparticles has been a long-standing challenge posed to chemists because of their relatively low redox potential and ease of oxidation when exposed to air. In the quest for new nanomaterials and applications in catalysis and sustainable protocols, some effective methods have been developed in our groups for the preparation of nanocatalysts.[5,20,21] Herein, we present the synthesis of monodisperse Cu nanoparticles by taking advantage of the synergetic effect of trioctylphosphine (TOP) and bromide ion (Br^-) in a disproportionation reaction. Then, a SiO₂@Cu nanocatalyst was synthesized by supporting the Cu nanoparticles on a silanized silica aerogel. The as-synthesized and well characterized SiO₂@Cu nanocatalyst was employed for A3 coupling reactions. The synthesis of propargylamines is one of the most demanded and valuable for various drug intermediates and other important valuable adducts.[22–24] Generally, propargylamines are prepared by stoichiometric amounts of traditional reagents, which produce waste at the end of the reaction, but in recent years, propargylamines have been synthesised by a new one-pot A3 coupling reaction, which gives only water as a by-product. Hence, this coupling synthesis of propargylamines is an important alternative reaction pathway. In addition, various methodologies for the catalytic synthesis of propargylamines have been recently reported.[25–34] However, in most of these methodologies, gold or silver catalysts were used in the A3 coupling reactions, which are expensive. From an economic point of view, replacing noble metal catalysts with low cost and robust transition metal catalysts with equal or similar activity is also crucial in green chemistry.[35]

Typically, CuBr was dissolved in oleylamine under strong magnetic stirring and Ar purging. After that, TOP was injected into the mixed solution rapidly, followed by stirring at 100 °C

aDepartment of Materials Science and Engineering, College of Materials, Xiamen University, Xiamen 361005, People's Republic of China. E-mail: dlpeng@xmu.edu.cn; Fax: +86 592 2183515; Tel: +86 592 2180155

bREQUIMTE, Department of Chemistry, Faculty of Science and Technology, New University of Lisbon, Quinta da Torre, 2829-516 Caparica, Lisbon, Portugal. E-mail: m.gawande@fct.unl.pt; Fax: +351 21 2948550; Tel: +351 96 4223243

† Electronic supplementary information (ESI) available: Experimental details, SEM and TEM images, BET data. See DOI: 10.1039/c3ra43341b

for 5 min and then heating up to 260 °C for the preparation of monodisperse Cu nanoparticles. By aging the mixed solution for 3 h, monodisperse Cu nanoparticles with an average diameter of 23 nm were obtained (see Fig. S1 in ESI† for more detailed information on size distribution). As demonstrated in the representative TEM image in Fig. 1a, the nanoparticles are all of spherical morphology with a narrow size distribution, indicating a good monodispersity on carbon grids. The selective area electron diffraction (SAED) pattern acquired from these Cu nanoparticles (Fig. 1b) exhibits a series of diffraction rings corresponding to the face-centered cubic (FCC) structure of Cu, and no other diffraction rings belonging to CuO are observed, illustrating the pure nature of the Cu nanoparticles. The freshly prepared Cu nanoparticles were collected by centrifugation and washed with a mixture of anhydrous hexane and acetone. After dispersion in a toluene solution *via* ultrasound sonication for 30 min, a bright reddish solution was obtained (Fig. 1c inset). The solution displays an absorption peak at 574 nm in the vis-NIR extinction spectrum (Fig. 1c) due to the surface plasmon resonance of the Cu nanoparticles. The sharp absorption peak also indicates the narrow size distribution of the Cu nanoparticles. These freshly prepared Cu nanoparticles could be assembled into a two dimensional superlattice on a carbon grid (Fig. 1d) or silicon wafer (Fig. S2†) *via* slow evaporation of the toluene solution of the Cu nanoparticles in a thermostat.

Furthermore, the synergetic or additive effect of TOP and Br⁻ was found to be necessary for the formation of monodisperse Cu nanoparticles. Control experiments were carried out to verify this conclusion. The blue solution of CuBr and oleylamine at 100 °C turned achromatous after the injection of TOP revealing the coordination between TOP and the Cu⁺ ions while, in the absence of TOP, a reddish solution was observed when the reaction temperature reached 210 °C, indicating the formation of Cu seed particles, which was a much lower temperature than
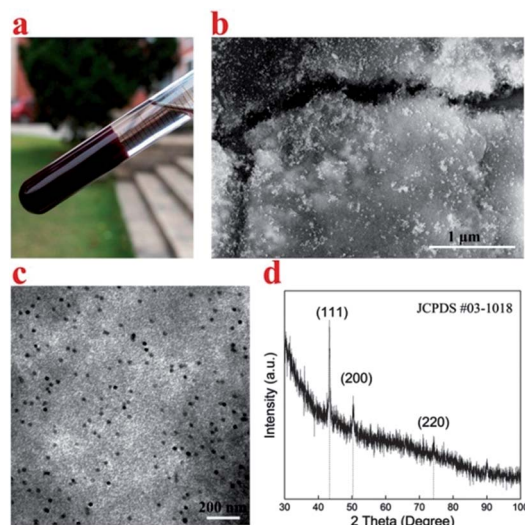

Fig. 2 SiO$_2$@Cu nanocatalyst. (a) Photography of the SiO$_2$@Cu nanocatalyst after 2 h standing in the toluene solution. (b) SEM image. (c) TEM image. (d) XRD pattern.

in the presence of TOP (it turned red at about 250 °C). The fast disproportionation reaction of Cu⁺ without the coordination of TOP resulted in large Cu nanocrystals with chaotic morphologies (Fig. S3†). Preventing the metal ions from fast reduction to Cu(0) seems to be necessary to accumulate enough reactant species to reach the critical nucleation concentration to achieve instantaneous nucleation, which is particularly important to obtain highly monodisperse Cu nanoparticles. The formation of Cu⁺–TOP complexes in the reaction solution hindered the disproportionation reaction even under highly favorable conditions (210 °C in oleylamine solution).[18] Similarly, by taking advantage of the coordination between Pt²⁺ and a surfactant, Lee *et al.* have successfully synthesized monodisperse polyhedral Pt nanocrystals.[36] Meanwhile, the Br⁻ ions from the CuBr precursor are essential as well. In our previous
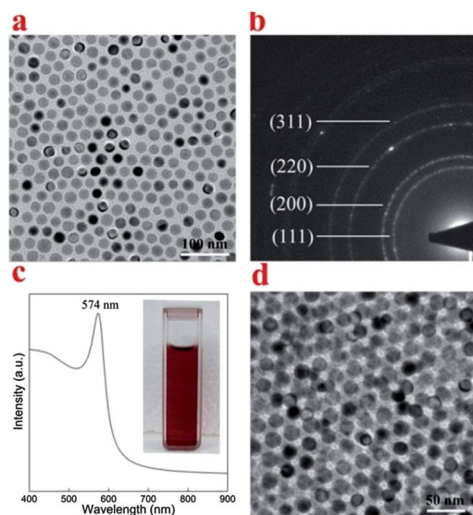

Fig. 1 Monodisperse Cu nanoparticles. (a) TEM image; (b) SAED pattern; (c) visible-NIR extinction spectrum of the Cu nanoparticles dissolved in toluene; (d) TEM image of the two dimensional supperlattice assembled on a carbon grid; inset in (c) shows the photography of the toluene solution of Cu nanoparticles.

Table 1 Optimization of the reaction conditions[a]

Entry	Catalyst	Solvent	Time (h)	Yield (%)
1	—	—	24	NR
2	SiO$_2$@Cu	CH$_3$CN	6	65
3	SiO$_2$@Cu	Water	12	30
4	SiO$_2$@Cu	Dioxane	7	60
5	SiO$_2$@Cu	AcOEt	7	58
6	SiO$_2$@Cu	Solvent-free	5	72
7	SiO$_2$@Cu	Toluene	5	95

[a] *Reaction conditions*: 4-methoxy benzaldehyde (1 mmol), phenyl acetylene (1.5 mmol), morpholine (1.1 mmol), SiO$_2$@Cu (50 mg), temperature 110 °C.
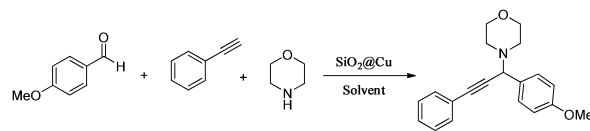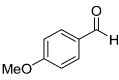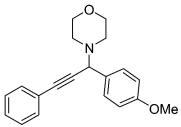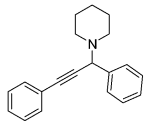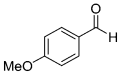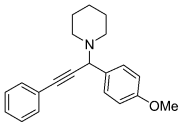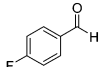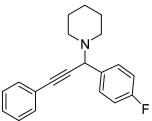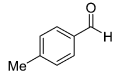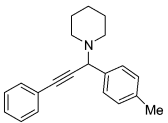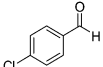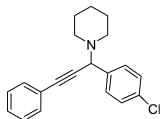
Table 2 SiO$_2$@Cu catalyzed A3 coupling reactions[a]

No.	Aldehyde	Amine	Product	Time (h)	Yield[b] (%) (TON)[c]
1				5	95 (1032)
2				5	94 (1021)
3				5	93 (1010)
4				6	86 (934)
5				6	82 (891)
6				6	85 (891)

[a] *Reaction conditions*: aldehyde (1 mmol), phenyl acetylene (1.5 mmol), amine (1.2 mmol), SiO$_2$@Cu (50 mg), toluene (1.5 mL), temp. 110 °C. [b] Isolated yield. [c] Turn over number.

studies, CuCl[37] and CuCl$_2$[38] were used as precursors to synthesize Cu nanowires or nanocubes in oleylamine solution. If we used Cu(NO$_3$)$_2$ instead of CuBr in the typical procedure without changing other factors, the Cu nanoparticles displayed a wide size distribution (Fig. S4†). This may be due to the adsorption of Br⁻ on the surface of the seed particles which ensures a slow and synchronous nanocrystal growth process.

We next supported the as-synthesized Cu nanoparticles on a silanized silica aerogel to fabricate an oleophilic SiO$_2$@Cu nanocatalyst (15 wt% Cu). The silica aerogel was dissolved in the toluene solution of Cu nanoparticles by ultrasound sonication (see ESI† for the catalyst preparation). After two hours standing, delamination was observed in the mixed solution. The contrast between the colorless supernate and the reddish colloid (Fig. 2a) indicates that all Cu nanoparticles have been adsorbed onto the SiO$_2$ support and that strong interactions between the Cu nanoparticles and the SiO$_2$ support have been formed. Fig. 2b and c display the representative SEM and TEM images of the Cu nanoparticles deposited on the SiO$_2$ support, respectively, from which a good dispersion of Cu nanoparticles is observed. The X-ray diffraction (XRD) pattern acquired from the as-prepared Cu nanocatalyst after exposure to air for one month shows a series of diffraction peaks in accordance with

FCC Cu (JCPDS #03-1018), revealing the high stability of this SiO$_2$@Cu nanocatalyst. The SiO$_2$@Cu nanocatalyst exhibits a relatively large Brunauer–Emmett–Teller (BET) specific surface area of 779.53 m^2 g^{-1} and many homogeneous mesopores (Fig. S5†).

The as-synthesized and well characterized SiO$_2$@Cu nanocatalyst was further investigated in A3 coupling reactions. The catalytic activity of SiO$_2$@Cu was initially tested for the model reaction between 4-methoxy benzaldehyde, phenyl acetylene and morpholine in various possible reaction conditions (Table 1).

First, we tested the reaction under catalyst-free and solvent-free conditions at room temperature and at 110 °C, but no product formation was observed (Table 1, entry 1). After optimization of the reaction conditions, it was noted that a fair yield was obtained under solvent-free conditions (Table 1, entry 6), but in toluene the yield of product was excellent (Table 1, entry 7). This could be attributed to the high dispersibility of SiO$_2$@Cu in toluene leading to a high surface area. In other solvents such as water, ethyl acetate, dioxane and acetonitrile, a low to moderate yield was observed (Table 1, entries 2–5) owing to the poor dispersibility of the SiO$_2$@Cu catalyst in polar solvents. Further exploration of the substrate scope of the A3 coupling reaction is depicted in Table 2.

Various aldehydes with morpholine and piperidine reacted with phenyl acetylene under optimized conditions to obtain the corresponding products in good to excellent yields (82–95%; Table 2). We believe that this reported protocol for the synthesis of propargylamines is cost effective (as it avoids using expensive metal gold) and the yields are comparable.[28,35]

A proposed mechanism for the A3 coupling reactions on the SiO_2@Cu nanocatalyst is depicted in Scheme 1 in the ESI.† The corresponding product is obtained *via* formation of copper acetylide, which has been proposed for A3 coupling reactions.[39] In a typical reaction mechanism, the C–H bond is activated by the copper species to give a copper acetylide intermediate (I), which reacts with the immonium ion (II) which is formed *in situ* from the aldehyde and the secondary amine to give the corresponding propargylamine (III) with elimination of a water molecule.

In summary, monodisperse Cu nanoparticles were synthesised in a facile one-pot procedure *via* a disproportionation reaction route. The synergetic or additive effect of TOP and Br$^-$ was found to be important in the formation of monodisperse Cu nanoparticles, which produces, by their coordination effect, an instantaneous nucleation and slow growth. By depositing the Cu nanoparticles on a SiO_2 support, an excellent catalytic performance in A3 coupling reactions for the synthesis of propargylamines was achieved with this high surface area SiO_2@Cu nanocatalyst. Further investigations are in progress in our laboratory.

Notes and references

1 Y. Xia, Y. J. Xiong, B. Lim and S. E. Skrabalak, *Angew. Chem., Int. Ed.*, 2009, **48**, 60–103.
2 N. N. Mallikarjuna and R. S. Varma, *Cryst. Growth Des.*, 2007, **7**, 686–690.
3 S.-W. Kim, M. Kim, W. Y. Lee and T. Hyeon, *J. Am. Chem. Soc.*, 2002, **124**, 7642–7643.
4 H. Shipley, K. Engates and A. Guettner, *J. Nanopart. Res.*, 2011, **13**, 2387–2397.
5 M. B. Gawande, P. S. Branco and R. S. Varma, *Chem. Soc. Rev.*, 2013, **42**, 3371–3393.
6 S. Jeong, K. Woo, D. Kim, S. Lim, J. S. Kim, H. Shin, Y. Xia and J. Moon, *Adv. Funct. Mater.*, 2008, **18**, 679–686.
7 J. L. Cuya Huaman, K. Sato, S. Kurita, T. Matsumoto and B. Jeyadevan, *J. Mater. Chem.*, 2011, **21**, 7062–7069.
8 H. Wu, L. Hu, M. W. Rowell, D. Kong, J. J. Cha, J. R. McDonough, J. Zhu, Y. Yang, M. D. McGehee and Y. Cui, *Nano Lett.*, 2010, **10**, 4242–4248.
9 A. R. Rathmell and B. J. Wiley, *Adv. Mater.*, 2011, **23**, 4798–4803.
10 J.-H. Lin and V. V. Guliants, *Appl. Catal., A*, 2012, **445–446**, 187.
11 B. Sarkar, *et al.*, *Green Chem.*, 2012, **14**, 2600–2606.
12 M. Kidwai, S. Bhardwaj, N. K. Mishra, A. Jain, A. Kumar and S. Mozzumdar, *Catal. Sci. Technol.*, 2011, **1**, 426–430.
13 B. C. Ranu, A. Saha and R. Jana, *Adv. Synth. Catal.*, 2007, **349**, 2690–2696.
14 Z. Peng and H. Yang, *Nano Today*, 2009, **4**, 143–164.
15 C. Li, K. L. Shuford, Q. H. Park, W. Cai, Y. Li, E. J. Lee and S. O. Cho, *Angew. Chem.*, 2007, **119**, 3328–3332.
16 R. Jin, Y. Cao, C. A. Mirkin, K. L. Kelly, G. C. Schatz and J. G. Zheng, *Science*, 2001, **294**, 1901–1903.
17 J. L. Cuya Huaman, K. Sato, S. Kurita, T. Matsumoto and B. Jeyadevan, *J. Mater. Chem.*, 2011, **21**, 7062.
18 A. R. Tao, S. Habas and P. Yang, *Small*, 2008, **4**, 310–325.
19 C. B. Murray, C. R. Kagan and M. G. Bawendi, *Annu. Rev. Mater. Sci.*, 2000, **30**, 545–610.
20 M. B. Gawande, P. S. Branco, I. D. Nogueira, C. A. A. Ghumman, N. Bundaleski, A. Santos, O. M. N. D. Teodoro and R. Luque, *Green Chem.*, 2013, **15**, 682–689.
21 H. Guo, Y. Chen, H. Ping, L. Wang and D.-L. Peng, *J. Mater. Chem.*, 2012, **22**, 8336–8344.
22 V. A. Peshkov, O. P. Pereshivko and E. V. Van der Eycken, *Chem. Soc. Rev.*, 2012, **41**, 3790–3807.
23 A. A. Boulton, B. A. Davis, D. A. Durden, L. E. Dyck, A. V. Juorio, X. M. Li, I. A. Paterson and P. H. Yu, *Drug Dev. Res.*, 1997, **42**, 150–156.
24 M. Miura, M. Enna, K. Okuro and M. Nomura, *J. Org. Chem.*, 1995, **60**, 4999–5004.
25 J. Dulle, K. Thirunavukkarasu, M. M. C. Mittelmeijer-Hazeleger, D. Andreeva, R. N. Shiju and G. Rothenberg, *Green Chem.*, 2013, **15**, 1238–1243.
26 G. Villaverde, A. Corma, M. Iglesias and F. Sanchez, *ACS Catal.*, 2012, **2**, 399–406.
27 K. K. R. Datta, B. V. S. Reddy, K. Ariga and A. Vinu, *Angew. Chem., Int. Ed.*, 2010, **49**, 5961–5965.
28 K. Layek, R. Chakravarti, M. L. Kantam, H. Maheswaran and A. Vinu, *Green Chem.*, 2011, **13**, 2878–2887.
29 K. M. Reddy, N. S. Babu, I. Suryanarayana, P. S. S. Prasad and N. Lingaiah, *Tetrahedron Lett.*, 2006, **47**, 7563–7566.
30 G. Shore, W. J. Yoo, C. J. Li and M. G. Organ, *Chem.–Eur. J.*, 2010, **16**, 126–133.
31 L. Lili, Z. Xin, G. Jinsen and X. Chunming, *Green Chem.*, 2012, **14**, 1710–1720.
32 C. M. Wei, Z. G. Li and C. J. Li, *Org. Lett.*, 2003, **5**, 4473–4475.
33 Z. G. Li, C. M. Wei, L. Chen, R. S. Varma and C. J. Li, *Tetrahedron Lett.*, 2004, **45**, 2443–2446.
34 C. M. Wei and C. J. Li, *J. Am. Chem. Soc.*, 2003, **125**, 9584–9585.
35 M. Kidwai, V. Bansal, A. Kumar and S. Mozumdar, *Green Chem.*, 2007, **9**, 742–745.
36 H. Lee, S. E. Habas, S. Kweskin, D. Butcher, G. A. Somorjai and P. Yang, *Angew. Chem.*, 2006, **118**, 7988–7992.
37 E. Ye, S. Zhang, S. Liu and M. Han, *Chem.–Eur. J.*, 2011, **17**, 3074.
38 H. Guo, Y. Chen, H. Ping, J. Jin and D. Peng, *Nanoscale*, 2013, **5**, 2394.
39 R. R. Julian, J. A. May, B. M. Stoltz and J. L. Beauchamp, *J. Am. Chem. Soc.*, 2003, **125**, 4478–4486.